

Generation of oxidant stress in cultured endothelial cells by methylene blue: protective effects of glucose and ascorbic acid

James M. May^{a,b,*}, Zhi-chao Qu^a, Richard R. Whitesell^b

^aDepartment of Medicine, 715 Preston Research Building, Vanderbilt University School of Medicine, Nashville, TN 37232-6303, USA

^bDepartment of Molecular Physiology and Biophysics, 704 Light Hall, Vanderbilt University School of Medicine, Nashville, TN 37232-6303, USA

Received 28 April 2003; accepted 6 June 2003

Abstract

The thiazine dye methylene blue has long been used to stimulate cellular redox metabolism. To determine the extent to which it also generates oxidant stress in cells, its effects in cultured human-derived endothelial cells were studied. As expected, low concentrations of the dye (2–20 μ M) activated the pentose phosphate pathway and oxidized both NADPH and NADH. Methylene blue enhanced extracellular ferricyanide reduction, indicating that the reduced form of the dye was present outside the cells. This reduction was greater when ferricyanide was added just before rather than 15 min after methylene blue, confirming that the dye is at least initially reduced at the cell surface. In the absence of glucose, methylene blue at concentrations above 5 μ M increased intracellular oxidant stress, as manifest by oxidation of dihydrofluorescein and cellular GSH. Inclusion of glucose protected against these effects. In cells that had been loaded with ascorbate, the dye caused progressive oxidation of ascorbate, even in the presence of D-glucose. Loading cells with ascorbate also partially prevented oxidation of dihydrofluorescein by methylene blue. These results suggest that concentrations of the dye above 5 μ M generated intracellular reactive oxygen species that were scavenged by ascorbate and GSH. Further, although D-glucose enhanced reduction of methylene blue, it ameliorated the oxidant stress generated by the dye.

© 2003 Elsevier Inc. All rights reserved.

Keywords: Methylene blue; Ascorbic acid; Ferricyanide; Dihydrofluorescein; Oxidant stress; EA.hy926 endothelial cells

1. Introduction

The redox dye methylene blue (MB^+) has long been used as a tool to dissect intracellular redox metabolism. Because of its size and positive charge, it is unlikely that the oxidized or “blue” MB^+ enters cells appreciably. Further, Merker and co-workers showed that cultured pulmonary endothelial cells reduce MB^+ at the cell surface *via* a novel trans-membrane thiazine reductase activity [1,2]. The resulting “leuko” or colorless form of methylene blue (MBH) is uncharged, lipophilic, and enters cells by diffusion across the plasma membrane where it is re-oxidized and thus sequestered within the cells [2,3]. Although molecular oxygen can directly oxidize MBH with generation of superoxide [4], reaction of MBH with heme-containing proteins

is greatly favored in cells [4,5]. In erythrocytes, MBH is directly oxidized by oxy- or methemoglobin [5–7]. In cells lacking hemoglobin, MBH oxidation appears to be mediated by other iron-containing proteins, such as cytochrome *c* [4], guanylate cyclase [8], nitric oxide synthase [9], and probably many others. However, if the capacity of the iron-containing proteins to fully oxidize MBH is overwhelmed, there is the potential for partial oxidation of MBH by molecular oxygen to form superoxide.

Redox cycling of intracellular MB^+ could further increase superoxide generation. To redox cycle, MB^+ would have to be reduced again within the cell. In erythrocytes, MB^+ is reduced *via* a poorly characterized NADPH dehydrogenase [7], termed diaphorase II [6]. In nucleated cells, MB^+ reduction has been demonstrated for heme-containing proteins, such as xanthine oxidase and cytochrome *c*-dependent reductases [4,10]. Although in endothelial cells the net effect of treatment with MB^+ is sequestration of MB^+ within as yet unknown organelles [2,3], redox cycling could still occur.

* Corresponding author. Tel.: +1-615-936-1653; fax: +1-615-936-1667.

E-mail address: james.may@vanderbilt.edu (J.M. May).

Abbreviations: KRH, Krebs–Ringer HEPES; MBH, reduced methylene blue; MB^+ , oxidized methylene blue; ROS, reactive oxygen species.

Despite the potential for redox cycling of MB^+ , evidence that it generates superoxide and other reactive oxygen species (ROS) within cells is indirect. Metz *et al.* [5] found that low concentrations of MB^+ ($<6\ \mu\text{M}$) added to human erythrocytes activated the pentose phosphate pathway, but did not increase oxygen consumption. However, higher MB^+ concentrations ($20\text{--}100\ \mu\text{M}$) not only increased the activity of the pentose phosphate pathway, but also increased oxygen consumption and oxidized GSH. The decrease in GSH was presumably due to scavenging of ROS generated by reaction of molecular oxygen with either MBH or its one-electron oxidized radical form. It remains to be demonstrated, however, that ROS are produced at high MB^+ concentrations.

In the present work, cellular metabolism and ROS generation by EA.hy926 endothelial cells were evaluated across a range of MB^+ concentrations. EA.hy926 is a permanent hybridoma cell line derived from human umbilical vein endothelial cells [11]. Endothelial cells were studied because they might be exposed to such concentrations of MB^+ during therapy of methemoglobinemia, as an antidote for paraquat poisoning [10], or during treatment of shock syndromes [12,13], and to determine their mechanisms for handling oxidant stress.

2. Materials and methods

2.1. Materials

EA.hy926 cells were generously provided by Dr. Cora Edgell (University of North Carolina, Chapel Hill, NC). Culture medium for the cells consisted of Dulbecco's minimal essential medium that contained 20 mM D-glucose, 5 mM hypoxanthine, 20 μM aminopterin, and 0.8 mM thymidine, and 10% (v/v) fetal bovine serum. The cells were cultured to confluence for 18–24 hr before use in an experiment. MB^+ and other analytical reagents were from Sigma/Aldrich. Molecular Probes supplied the dihydrofluorescein diacetate. The latter was prepared to a 10 mM concentration in dimethylsulfoxide and stored at -20° until dilution for use in modified Krebs–Ringer buffer containing HEPES to maintain pH (KRH: 20 mM HEPES, 128 mM NaCl, 5.2 mM KCl, 1 mM NaH_2PO_4 , 1.4 mM MgSO_4 , and 1.4 mM CaCl_2 , pH 7.4). Radionuclides were purchased from New England Nuclear Life Science Products Inc.

2.2. Assay of radiolabeled glucose metabolism in EA.hy926 cells

Glucose metabolism beyond phosphorylation was assessed as the release of $^3\text{H}_2\text{O}$ from D-[2- ^3H]glucose [14]. Pentose phosphate pathway activity was measured as recently described by measuring $^{14}\text{CO}_2$ release from D-[1- ^{14}C]glucose using a high throughput 96-well microtiter

plate method [15]. To test the effect of MB^+ on glucose utilization, the indicated concentration of MB^+ was added just before incubation with radionuclides. The activity of the pentose phosphate pathway was calculated by subtracting the nmol of $^{14}\text{CO}_2$ generated from D-[6- ^{14}C]glucose (which reflects activity of the tricarboxylic acid cycle) from that generated from D-[1- ^{14}C]glucose.

2.3. Intracellular oxidant stress measured by oxidation of dihydrofluorescein

Intracellular ROS were measured as oxidation of intracellular dihydrofluorescein, as previously described [15]. Briefly, EA.hy926 cells in 96-well plates were rinsed twice in KRH to remove culture medium, and incubated in 0.2 mL of KRH that contained 5 mM glucose, 20 μM dihydrofluorescein diacetate, and other additives as noted. The cells were incubated for 30 min at 37° , rinsed three times with 0.2 mL of KRH, and then incubated further in 0.2 mL of KRH that contained 5 mM glucose and the indicated concentration of MB^+ . The plate was loaded into a Fluostar Galaxy fluorescence microtiter plate reader and incubated at 37° for 33 min with measurement of the fluorescence in each well every 4 min. The excitation wavelength was 480 nm, and the emission wavelength was 520 nm.

2.4. Other assays

Intracellular concentrations of GSH were measured using the method of Hissin and Hilf [16] as previously described [17]. The recycling method of Zerez *et al.* [18] was used to measure pyridine nucleotide concentrations in 1 mL lysates from cells cultured in 6-well plates. In this assay, cells in 6-well plates are treated with 1 mL of ice-cold lysis buffer containing 20 mM NaHCO_3 , 100 mM Na_2CO_3 , and 10 mM nicotinamide, frozen on dry ice, and allowed to thaw on ice. The cell material is scraped from the plate, microfuged for 5 min at 3° to remove particulate matter, and the extracts are assayed for pyridine nucleotides as described [18]. The assay uses alcohol dehydrogenase to measure NADH, and glucose 6-phosphate dehydrogenase to measure NADPH. It employs a heating step of 60° for 30 min to destroy NAD(P)^+ , so that the reduced forms of the pyridine nucleotides can be selectively measured. The heating step also frees protein-bound NAD(P)H , so that total cell nucleotides are measured. Intracellular ascorbate was measured as previously described [19] using high performance liquid chromatography with electrochemical detection [20], except that tetrapentylammonium bromide was used as an ion pair reagent. Intracellular concentrations of GSH, pyridine nucleotides, and ascorbate were expressed relative to the intracellular distribution space of 3-O-[^{14}C]methylglucose, which was taken as $3.6 \pm 1.2\ \mu\text{L/mg protein}$ [15]. Potassium ferricyanide ($\text{C}_6\text{FeK}_3\text{N}_6$) reduction was measured by

the *ortho*-phenanthroline method of Avron and Shavit [21], with correction in each assay for the absorbance generated in the presence of cells by the same concentration of MB^+ without ferricyanide in a paired sample. This value was less than 20% of that observed in the presence of ferricyanide.

2.5. Data analysis

Results are shown as mean \pm SE. Differences between treatments were analyzed with the computer program SigmaStat 2.0. Comparison of two treatments was made using the non-paired Student's *t*-test. Comparisons of more than two treatments were made using either one- or two-way ANOVA with *post hoc* testing by Dunnett's test, as appropriate. A value of $P < 0.05$ was considered significant.

3. Results

The ability MB^+ to enhance glucose utilization was studied, with the results shown in Fig. 1. Incubation of EA.hy926 cells with increasing amounts of MB^+ for 30 min in KRH buffer containing various concentrations of D-[1- ^{14}C]glucose resulted in progressive increases in $^{14}\text{CO}_2$ release (Fig. 1A). This increase was evident across the range of glucose concentrations employed, indicating that the effect of MB^+ to enhance oxidation does not depend on the energy state of the cell. However, MB^+ did not affect the appearance of $^3\text{H}_2\text{O}$ from any concentration of [2- ^3H]glucose in the same incubations (Fig. 1B). The latter assay measures glucose utilization beyond glucose 6-phosphate. Release of $^{14}\text{CO}_2$ did not increase

linearly with increasing amounts of MB^+ at any glucose concentration (Fig. 1A). This suggests that there are limits to activation of pentose phosphate pathway activity by MB^+ in these cells, even at low glucose concentrations.

The major stimulus for activation of the pentose phosphate pathway by MB^+ is conversion of NADPH to NADP^+ . NADP^+ is a co-factor for and enhances the activity of glucose 6-phosphate dehydrogenase, the rate-limiting enzyme of the pathway. As shown in Fig. 2, concentrations of both NADPH and NADH decreased by about 50% at even the lowest concentration of MB^+ used. As indicated by the size of the error bars in Fig. 2, there was variability in day-to-day measurements in basal levels of NAD(P)H, but the effect of MB^+ was consistent in each experiment performed. Direct oxidation of NAD(P)H by MB^+ in KRH in the absence of cells was observed as a decrease in spectrophotometric absorbance at 340 nm (results not shown). Thus, any intracellular MB^+ might have contributed to decreases in NAD(P)H directly.

Another estimate of the ability of these cells to reduce or recycle MB^+ was obtained by following the reduction of extracellular ferricyanide by MBH [2]. Because of its size and charge, ferricyanide does not enter cells during the incubation times used in these studies [22]. Thus, ferricyanide reduction can be used as an estimate for the integrated ability of the cells to reduce MB^+ . Cells were treated with increasing concentrations of MB^+ in the presence of 1 mM ferricyanide for 30 min, with the results that extracellular reduced ferricyanide increased linearly with MB^+ (Fig. 3, circles). When cells were first incubated for 15 min with MB^+ , increases in ferricyanide reduction were not evident at MB^+ concentrations below 50 μM , and ferricyanide reduction was significantly decreased over the

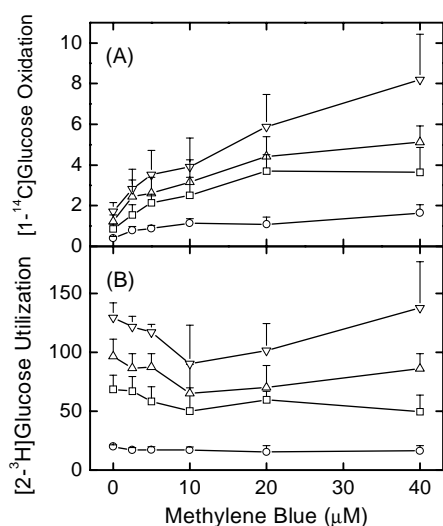


Fig. 1. MB^+ effects on glucose metabolism by EA.hy926 cells. Conversion of D-[1- ^{14}C]glucose to $^{14}\text{CO}_2$ (A) and of [2- ^3H]glucose to $^3\text{H}_2\text{O}$ (B) was measured as described in Section 2 at the following concentrations of D-glucose: circles, 0.16 mM; squares, 0.63 mM; triangles, 1.25 mM; and inverted triangles, 2.5 mM. Units for both activities are nmol/mg protein/30 min. Results are shown as mean \pm SE from four experiments.

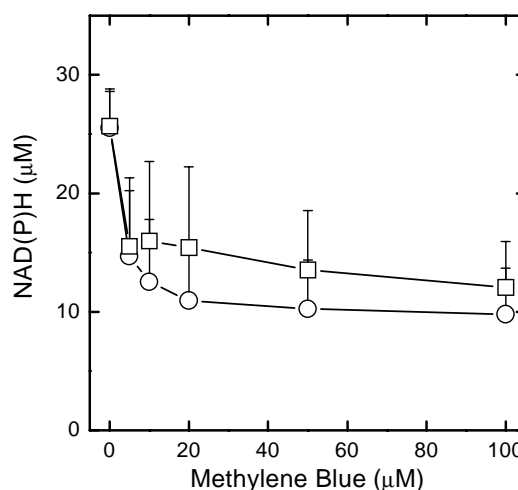


Fig. 2. Decreases in cellular pyridine nucleotide concentrations due to MB^+ . EA.hy926 cells in 6-well plates were incubated at 37° in culture medium that contained the indicated concentration of MB^+ . After 15 min, the medium was removed and the cells were rinsed twice with KRH and taken for assay of NADPH (circles) and NADH (squares). Results are shown as mean \pm SE from four experiments with each nucleotide. For each nucleotide, all points were significantly different from control without added MB^+ .

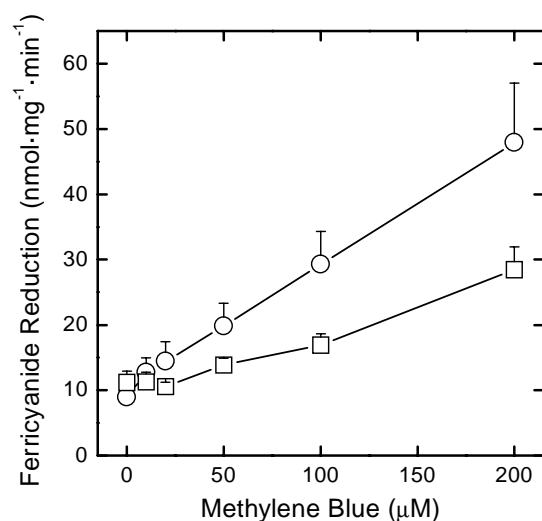


Fig. 3. Stimulation of ferricyanide reduction by MB^+ . EA.hy926 cells in 12-well plates were incubated at 37° in KRH that contained 5 mM D-glucose. In experiments shown by the circles ($N = 9$), 1 mM ferricyanide was added first, followed by the indicated concentration of MB^+ . All increases due to MB^+ were significant compared to cells not incubated with MB^+ by one-way ANOVA. In experiments shown by the squares ($N = 5$), MB^+ was added first for 15 min, followed by ferricyanide. Significant increases were present only above $50 \mu\text{M}$ MB^+ by one-way ANOVA. For both protocols, after 30 min of incubation with ferricyanide, duplicate aliquots of the medium were removed for assay of ferrocyanide. The averaged slopes of the lines for the two types of experiment were different by non-paired t -testing.

range of MB^+ concentrations utilized (Fig. 3, squares). This effect was likely due in part to decreased MBH outside the cells following preincubation with MB^+ , since a 15-min preincubation at 37° of EA.hy926 cells with $10 \mu\text{M}$ MB^+ before addition of 1 mM ferricyanide decreased extracellular MB^+ (measured as the optical density at 610 nm) by $13 \pm 0.6\%$ compared to cells treated for 15 min with both ferricyanide and MB^+ ($N = 5$, $P = 0.01$).

To determine whether MB^+ reduction is associated with generation of intracellular ROS, generation of the latter within cells was measured as the oxidation of dihydrofluorescein to fluorescein. In this experiment, cells were first incubated with dihydrofluorescein diacetate, which diffuses into the cells and is trapped following removal of the two acetate groups by cellular esterases. After rinsing the cells to remove extracellular dye, MB^+ was added and the increase in fluorescence was followed over 34 min in a fluorescence microtiter plate reader. As shown in Fig. 4A, after a lag-phase, MB^+ increased fluorescence in a time-dependent manner. When the slope of the linear portion of the time course was calculated for several experiments, the results shown in Fig. 4B were obtained. In cells incubated in the absence of D-glucose (squares), an increase in fluorescence was apparent at $5 \mu\text{M}$ MB^+ , with a plateau above $50 \mu\text{M}$ MB^+ . The presence of 5 mM D-glucose inhibited the oxidation of dihydrofluorescein. MB^+ alone did not directly oxidize

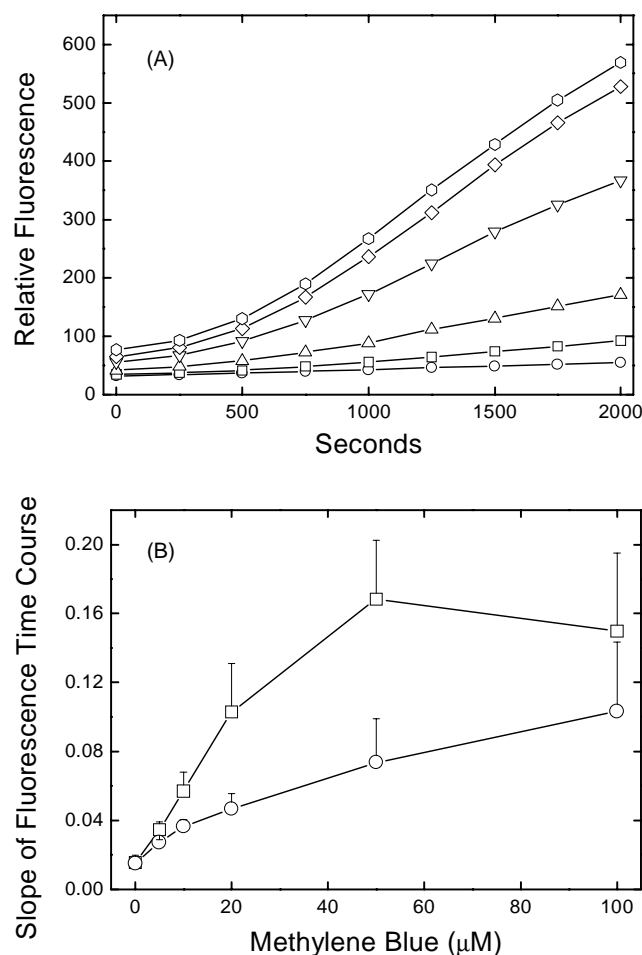


Fig. 4. Stimulation of dihydrofluorescein oxidation by MB^+ in EA.hy926 cells. (A) EA.hy926 cells in 96-well plates were loaded with dihydrofluorescein as described under Section 2 in the absence of 5 mM D-glucose. After rinsing with KRH to remove extracellular dye, the cells were treated in KRH in the absence of glucose with one of the following concentrations of MB^+ : no MB^+ , circles; $5 \mu\text{M}$, squares; $10 \mu\text{M}$, triangles; $20 \mu\text{M}$, inverted triangles; $50 \mu\text{M}$, diamonds; $100 \mu\text{M}$, hexagons. Changes in fluorescence were measured in 4 wells and the average is shown for each time point. (B) Assay conditions were as in panel A, except that cells were incubated with (circles) or without (squares) 5 mM D-glucose during the entire experiment. The linear slope of the fluorescence increase (from 750 s) is shown for four experiments. The two curves were significantly different from each other ($P < 0.05$).

dihydrofluorescein (results not shown). Thus, MB^+ -induced generation of ROS within the cells was apparent at concentrations as low as $5 \mu\text{M}$, and was blunted in the presence of glucose.

To further assess the extent to which EA.hy926 cells were under oxidant stress from MB^+ , intracellular concentrations of GSH were measured. In the presence of 5 mM D-glucose, increasing amounts of MB^+ did not affect intracellular GSH concentrations (Fig. 5). However, when D-glucose was omitted from the medium during the incubation, GSH concentrations in the cells decreased in a linear manner to reach about 50% of control at $100 \mu\text{M}$ MB^+ . Thus, D-glucose was required to prevent oxidation of GSH due to MB^+ , an effect that became significant over the same

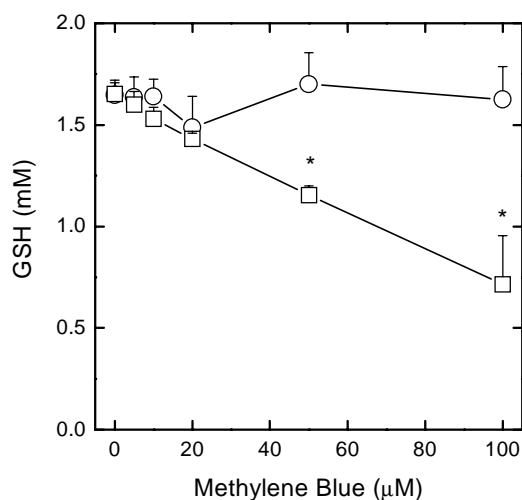


Fig. 5. Preservation of GSH in MB⁺-treated EA.hy926 cells by glucose. Cells in 6-well plates were incubated in KRH at 37° with the indicated concentration of MB⁺ in the presence (circles) or absence (squares) of 5 mM D-glucose. After 15 min, the cells were rinsed and taken for assay of intracellular GSH. Results are shown as mean ± SE from at least four experiments for each glucose condition, with an asterisk indicating $P < 0.05$ compared to the sample not treated with MB⁺.

range of MB⁺ concentrations over which D-glucose also decreased dihydrofluorescein oxidation (Fig. 4). Since GSH does not directly reduce MB⁺ (results not shown), these results suggest that GSH was oxidized by ROS generated from MB⁺ metabolism, or that GSH recycling was impaired by decreased availability of NADPH at glutathione reductase, or both.

Additional support for generation of ROS by high concentrations of MB⁺ was found by measuring changes in ascorbate in cells acutely loaded with ascorbate by incubation with dehydroascorbic acid. The latter was accomplished by incubating cells with increasing amounts of MB⁺ in the presence of 0.5 mM dehydroascorbic acid and 5 mM D-glucose. Although the cells had negligible intracellular ascorbate in the absence of loading (results not shown), a 15-min incubation with dehydroascorbic acid increased intracellular ascorbate to over 2.5 mM (Fig. 6A). Intracellular ascorbate concentrations progressively decreased following incubation with increasing concentrations of MB⁺, reaching about 30% of control at 100 μM MB⁺ (Fig. 6A). GSH concentrations did not change significantly under these conditions (Fig. 6B). Similar results were observed when cells were preincubated for 15 min with dehydroascorbic acid before addition of MB⁺ (results not shown), so MB⁺ was not simply preventing reduction of dehydroascorbic acid to ascorbate. The possibility was considered that the effect of MB⁺ to decrease intracellular ascorbate was due to direct reaction. Incubation of 50 μM concentrations of MB⁺ and ascorbate for 15 min at 37° in KRH resulted in the loss of 14 ± 5% of ascorbate compared to 5 ± 1% of an untreated ascorbate sample (N = 3). This small decrease suggests that direct reaction may account for some, but not all of the decrease in intracellular ascorbate observed.

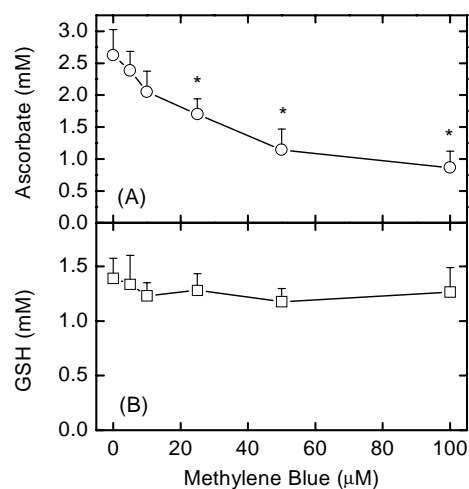


Fig. 6. Decreases in intracellular ascorbate caused by MB⁺. EA.hy926 cells in 6-well plates were incubated at 37° in KRH that contained 5 mM D-glucose, 0.5 mM dehydroascorbic acid, and the indicated concentration of MB⁺. After 15 min, the medium was removed and the cells were rinsed twice in KRH and taken for assay of intracellular ascorbate (A) and GSH (B). Results are shown as mean ± SE from three experiments, with an asterisk indicating $P < 0.05$ compared to the sample not exposed to MB⁺.

In cells containing ascorbate, oxidation of dihydrofluorescein was decreased compared to cells not containing ascorbate, although the effect was relatively modest (Fig. 7). These results suggest that ascorbate is more sensitive to ROS generated by MB⁺ than is GSH, and support the notion that high concentrations of MB⁺

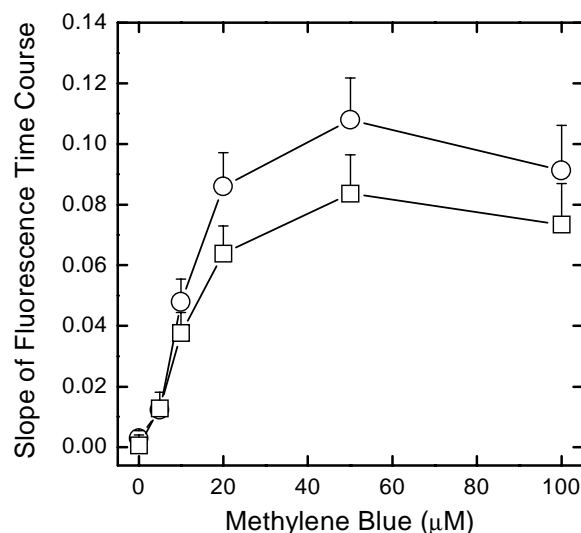


Fig. 7. Effects of ascorbate loading on MB⁺-induced oxidation of dihydrofluorescein. EA.hy926 cells in 96-well plates were loaded with dihydrofluorescein at 37° in KRH that contained 5 mM D-glucose in the absence (circles) or presence (squares) of 0.5 mM dehydroascorbic acid. After 30 min, the cells were rinsed with KRH and incubated in KRH containing 5 mM D-glucose and the indicated concentration of MB⁺ during measurement of fluorescence in a microtiter plate reader. Results from five experiments are shown as mean ± SE of the linear slope of the time course of fluorescence increase. The two curves are significantly different from each other ($P < 0.05$).

generated an oxidant stress that was partially blunted by the presence of intracellular reducing equivalents, this time in the form of ascorbate.

4. Discussion

4.1. Cellular mechanisms of MB^+ reduction

As expected from previous studies in erythrocytes [5,23], low concentrations of MB^+ activated the pentose phosphate pathway in EA.hy926 endothelial cells (Fig. 1). It is perhaps surprising that glucose utilization beyond generation of glucose 6-phosphate was not increased by MB^+ . This reflects the relatively small component of overall glucose utilization contributed by even an activated pentose phosphate pathway. In the present studies this was typically less than 10%. In other words, MB^+ is relatively specific in its activation of the pentose phosphate pathway as opposed to other pathways of glucose utilization in these cells.

The stimulus for pentose phosphate pathway activation was likely due to the increase in $NADP^+$ caused by reduction of MB^+ , which is reflected in the decrease in NADPH measured in these studies (Fig. 2). $NADP^+$ activates glucose 6-phosphate dehydrogenase, the rate-determining enzyme in the pentose phosphate pathway [23]. Since MB^+ is initially reduced at the cell surface by a trans-membrane thiazine dye reductase [1,2], the oxidation of NADPH could mean that it is a substrate for this activity. Similarly, the finding that NADH was also decreased may reflect a role for NADH as an electron donor for the reductase. Failure of NAD(P)H to decrease below 50% suggests that trans-membrane transfer of reducing equivalents to extracellular MB^+ was saturated. Also, since MB^+ is also found in endothelial cells after exposure to extracellular MB^+ [2], it could also mean that some NAD(P)H (e.g. bound to enzymes) was inaccessible to intracellular MB^+ . A similar shift in the cellular pyridine nucleotide redox state was first suggested by the results of Merker *et al.* [24], who reported that intracellular ratios of NAD(P)H/NAD(P) $^+$ correlated inversely with extracellular reduction of a polymer of the redox dye toluidine blue. Alternatively, since MBH generated at the cell surface diffuses into cells where it is re-oxidized to MB^+ [2], redox cycling within the cells could depend on the reducing capacity of heme-containing enzymes dependent on either NADPH or NADH, such as the cytochrome *c* reductases [10].

4.2. Site of MB^+ reduction

The experiments with ferricyanide support the conclusions of Merker and co-workers [1,2] that MBH is generated from MB^+ by a trans-membrane thiazine dye reductase at the exofacial cell surface. However, since ferricyanide is not reduced by the trans-membrane thiazine dye reductase [1,2], extracellular ferricyanide reduction

will not detect intracellular redox cycling of MB^+ . Thus, it provides only a minimal estimate of total MBH generation. Rates of ferricyanide reduction were lower when cells were preincubated with MB^+ than when ferricyanide was added just before MB^+ (Fig. 3). This would be the expected result if MBH generated at the cell surface diffuses into cells during a preincubation, so that less of the reduced form is accessible to ferricyanide added later. In contrast, ferricyanide added just before MB^+ will be continuously reduced by any MBH generated at the cell surface. Further, the failure of cells preincubated with MB^+ concentrations below 50 μM to enhance ferricyanide reduction in MBH-loaded cells suggests that little MBH escapes the cells until intracellular re-oxidation mechanisms are overwhelmed. These results support the concept that MB^+ is reduced on the outside surface of cells.

4.3. Generation of oxidant stress by MB^+

At concentrations of 5 μM and greater, MB^+ increases cellular oxidation of dihydrofluorescein, an effect that is partially prevented by including glucose in the incubation medium (Fig. 4). That glucose prevents generation of intracellular ROS is further suggested by the finding that it prevented oxidation of cellular GSH due to MB^+ (Fig. 5). Whereas one might think that glucose would enhance redox cycling of MB^+ with a resulting increase in intracellular ROS, the net effect of reducing equivalents provided by glucose is to decrease ROS capable of oxidizing dihydrofluorescein. Similar results were obtained when cells were pre-loaded with ascorbate by incubation with dehydroascorbic acid, in that ascorbate concentrations were decreased by MB^+ (Fig. 6), and ascorbate decreased dihydrofluorescein oxidation (Fig. 7). Although ascorbate can be directly oxidized by MB^+ , the present results suggest that most of the effect of ascorbate was to scavenge intracellular ROS generated by MB^+ , even when these were decreased by the presence of glucose.

Several possible causes of ROS generation by MB^+ in EA.hy926 cells can be considered. It is possible that they derive from the shift in redox balance of the cells generated from the initial extracellular reduction of MB^+ by the trans-membrane thiazine dye reductase. This redox shift might impair scavenging of ROS generated during normal mitochondrial metabolism [25]. Since neither pyridine nucleotides (Fig. 2) nor GSH (Fig. 5) are severely depleted by MB^+ (Fig. 2), this does not seem very likely. It is more likely that high intracellular MBH concentrations overwhelm the capacity of heme-containing enzymes and proteins to oxidize MBH, leaving MBH or its partially oxidized radical to react with molecular oxygen to form superoxide [4]. This mechanism was first suggested by the observations of Metz *et al.* [5], who showed that MB^+ concentrations above 5 μM increased oxygen consumption in erythrocytes. The present results more directly implicate superoxide, which is detected by dihydrofluorescein oxidation due to

several of its breakdown products in the cells [26]. Redox cycling of MB^+ might also contribute to ROS generation by maintaining intracellular MBH at high levels. However, redox cycling probably contributes little to ROS generation from MBH for two reasons. First, Merker *et al.* [2] showed that although pulmonary endothelial cells remove MB^+ from the medium as MBH, they accumulate MB^+ in precipitates in as yet unidentified organelles. That is, the cells preferentially oxidize MBH and the resulting MB^+ is sequestered, not reduced. Second, the present results show that glucose inhibited ROS generation due to MB^+ (Fig. 4B). Glucose was recently found to enhance ROS generation by menadione [27], an accepted redox cycling agent. The opposite behavior of MB^+ , despite its ability to enhance pentose phosphate pathway activity, suggests that MB^+ does not undergo redox cycling in endothelial cells. Rather, it is when excess MBH is partially oxidized by molecular oxygen rather than fully oxidized by heme proteins that it generates ROS.

4.4. Physiologic relevance of ROS generation by MB^+

Intravenous MB^+ has long been used to treat methemoglobinemia [28]. More recent uses have been to treat ifosfamide encephalopathy [29,30], and to inhibit nitric oxide release and maintain blood pressure in septic shock [12] and orthotopic liver transplantation [13]. The accepted mechanism is that cells reduce MB^+ to MBH, which then reduces Fe^{3+} to Fe^{2+} in the appropriate protein. This protein would be methemoglobin for methemoglobinemia [28], monoamine oxidase for ifosfamide encephalopathy [29], and endothelial nitric oxide synthase [9] and/or guanylate cyclase [8] (for inhibition of nitric oxide synthesis/action, respectively). Administration of a bolus injection of 100 mg MB^+ to humans results in a mean plasma concentration of 5 μM [29]. Since typical doses are 1.5–2 mg/kg [12,13], this or even higher plasma concentrations are likely to be present at least transiently. Toxicity has been reported with MB^+ administration [31,32], although there appears to be a relatively wide margin of safety [31]. The present results suggest that ROS may contribute to MB^+ toxicity in endothelial cells, especially when glucose metabolism is impaired, such as in deficiency of glucose 6-phosphate dehydrogenase [29].

Acknowledgment

This work was supported by NIH Grant DK 50435.

References

- [1] Bongard RD, Merker MP, Shundo R, Okamoto Y, Roerig DL, Linehan JH, Dawson CA. Reduction of thiazine dyes by bovine pulmonary arterial endothelial cells in culture. *Am J Physiol* 1995;269:L78–84.
- [2] Merker MP, Bongard RD, Linehan JH, Okamoto Y, Vyprachticky D, Brantmeier BM, Roerig DL, Dawson CA. Pulmonary endothelial thiazine uptake: separation of cell surface reduction from intracellular reoxidation. *Am J Physiol* 1997;272:L673–80.
- [3] Olson LE, Merker MP, Patel MK, Bongard RD, Daum JM, Johns RA, Dawson CA. Cyanide increases reduction but decreases sequestration of methylene blue by endothelial cells. *Ann Biomed Eng* 2000;28:85–93.
- [4] McCord JM, Fridovich I. The utility of superoxide dismutase in studying free radical reactions. II. The mechanism of the mediation of cytochrome *c* reduction by a variety of electron carriers. *J Biol Chem* 1970;245:1374–7.
- [5] Metz EN, Balcerzak SP, Sagone Jr AL. Mechanisms of methylene blue stimulation of the hexose monophosphate shunt in erythrocytes. *J Clin Invest* 1976;58:797–802.
- [6] Baird JK. Methylene blue-mediated hexose monophosphate shunt stimulation in human red blood cells in vitro: independence from intracellular oxidative injury. *Int J Biochem* 1984;16:1053–8.
- [7] Sass MD, Caruso CJ, Axelrod DR. Mechanism of the TPNH-linked reduction of methemoglobin by methylene blue. *Clin Chim Acta* 1969;24:77–85.
- [8] Gruetter CA, Kadowitz PJ, Ignarro LJ. Methylene blue inhibits coronary arterial relaxation and guanylate cyclase activation by nitroglycerin, sodium nitrite, and amyl nitrite. *Can J Physiol Pharmacol* 1981;59:150–6.
- [9] Mayer B, Brunner F, Schmidt K. Inhibition of nitric oxide synthesis by methylene blue. *Biochem Pharmacol* 1993;45:367–74.
- [10] Kelner MJ, Bagnell R, Hale B, Alexander NM. Methylene blue competes with paraquat for reduction by flavo-enzymes resulting in decreased superoxide production in the presence of heme proteins. *Arch Biochem Biophys* 1988;262:422–6.
- [11] Edgell CJ, McDonald CC, Graham JB. Permanent cell line expressing human factor VIII-related antigen established by hybridization. *Proc Natl Acad Sci USA* 1983;80:3734–7.
- [12] Preiser JC, Lejeune P, Roman A, Carlier E, De Backer D, Leeman M, Kahn RJ, Vincent JL. Methylene blue administration in septic shock: a clinical trial. *Crit Care Med* 1995;23:259–64.
- [13] Koelzow H, Gedney JA, Baumann J, Snook NJ, Bellamy MC. The effect of methylene blue on the hemodynamic changes during ischemia reperfusion injury in orthotopic liver transplantation. *Anesth Analg* 2002;94:824–9 [table].
- [14] Perriott LM, Kono T, Whitesell RR, Knobel SM, Piston DW, Granner DK, Powers AC, May JM. Glucose uptake and metabolism by cultured human skeletal muscle cells: rate-limiting steps. *Am J Physiol Endocrinol Metab* 2001;281:E72–80.
- [15] Jones W, Li X, Perriott LM, Whitesell RR, May JM. Uptake, recycling, and antioxidant functions of α -lipoic acid in endothelial cells. *Free Radic Biol Med* 2002;33:83–93.
- [16] Hissin PJ, Hilf R. A fluorometric method for determination of oxidized and reduced glutathione in tissues. *Anal Biochem* 1976;74:214–26.
- [17] May JM, Qu ZC, Li X. Requirement for GSH in recycling of ascorbic acid in endothelial cells. *Biochem Pharmacol* 2001;62:873–81.
- [18] Zerez CR, Lee SJ, Tanaka KR. Spectrophotometric determination of oxidized and reduced pyridine nucleotides in erythrocytes using a single extraction procedure. *Anal Biochem* 1987;164:367–73.
- [19] Li X, Hill KE, Burk RF, May JM. GSH is required to recycle ascorbic acid in cultured liver cell lines. *Antioxid Redox Signal* 2001;3:1089–97.
- [20] May JM, Qu Z-C, Mendiratta S. Protection and recycling of α -tocopherol in human erythrocytes by intracellular ascorbic acid. *Arch Biochem Biophys* 1998;349:281–9.
- [21] Avron M, Shavit N. A sensitive and simple method for determination of ferrocyanide. *Anal Biochem* 1963;6:549–54.
- [22] Székely M, Mátyai S, Straub FB. Über den Mechanismus der osmotischen Hämolyse. *Acta Physiol Acad Sci Hung* 1952;3:571–83.

- [23] Rose IA, O'Connell EL. The role of glucose 6-phosphate in the regulation of glucose metabolism in human erythrocytes. *J Biol Chem* 1964;239:12–7.
- [24] Merker MP, Bongard RD, Kettenhofen NJ, Okamoto Y, Dawson CA. Intracellular redox status affects transplasma membrane electron transport in pulmonary arterial endothelial cells. *Am J Physiol Lung Cell Mol Physiol* 2002;282:L36–43.
- [25] Kowaltowski AJ, Vercesi AE. Reactive oxygen generation by mitochondria. In: Lemasters JJ, Nieminen A-L, editors. *Mitochondria in pathogenesis*. New York: Kluwer Academic/Plenum Publishers; 2001. p. 281–300.
- [26] Hempel SL, Buettner GR, O'Malley YQ, Wessels DA, Flaherty DM. Dihydrofluorescein diacetate is superior for detecting intracellular oxidants: comparison with 2',7'-dichlorodihydrofluorescein diacetate, 5(and 6)-carboxy-2',7'-dichlorodihydrofluorescein diacetate, and dihydrorhodamine 123. *Free Radic Biol Med* 1999;27: 146–59.
- [27] May JM, Qu Z-C, Li X. Ascorbic acid blunts oxidant stress due to menadione in endothelial cells. *Arch Biochem Biophys* 2003;411: 136–44.
- [28] Wright RO, Lewander WJ, Woolf AD. Methemoglobinemia: etiology, pharmacology, and clinical management. *Ann Emerg Med* 1999;34: 646–56.
- [29] Aeschlimann C, Cerny T, Küpfer A. Inhibition of (mono)amine oxidase activity and prevention of ifosfamide encephalopathy by methylene blue. *Drug Metab Dispos* 1996;24:1336–9.
- [30] Küpfer A, Aeschlimann C, Cerny T. Methylene blue and the neurotoxic mechanisms of ifosfamide encephalopathy. *Eur J Clin Pharmacol* 1996;50:249–52.
- [31] Golubuff N, Wheaton R. Methylene blue induced cyanosis and acute hemolytic anemia complicating the treatment of methemoglobinemia. *J Pediatr* 1961;58:86–9.
- [32] Sills MR, Zinkham WH. Methylene blue-induced Heinz body hemolytic anemia. *Arch Pediatr Adolesc Med* 1994;148:306–10.